INT. J. REMOTE SENSING, 2001, VOL. 22, NO. 2 & 3, 315–338

The identification of phytoplankton pigments from absorption spectra

R. AGUIRRE-GÓMEZ†, A. R. WEEKS‡§ and S. R. BOXALL‖

†Instituto de Geografia, Universidad Nacional Autonoma de Mexico, Circuito Exterior, C.P. 4510, Coyoacan, D.F. Mexico
‡Maritime Faculty, Southampton Institute, East Park Terrace, Southampton SO14 OYN, England, UK
‖ University of Southampton, Department of Oceanography, Southampton Oceanography Centre, Waterfront Campus, European Way, Southampton SO17 1BJ, England, UK

(*Received 30 September 1998; in final form 1 July 1999*)

Abstract. The absorption spectra of photosynthetic algae are characterized by a continuous envelope, which is a result of the overlapping spectra of the indivual pigments. This feature makes it difficult to estimate the contribution of each pigment to the total absorption spectra. Derivative analysis is an objective tool for isolating absorption peaks in phytoplankton. Theoretically, electrons and ions of interacting molecules can be regarded as simple harmonic oscillators in an electromagnetic field, which result in a Lorentzian shape. However, when measured by an optical spectrophotometer the signal is transformed into a Gaussian curve. Thus, a combination of both types of curve provides a realistic approach to the decomposition of absorption spectra. In this study derivative analysis is performed on absorption spectra in order to prove that the method can be successfully used to identify the individual absorption spectra of component pigments. The spectra used are modelled phytoplankton, spectrophotometric measurements of algal cultures and samples from natural waters. A combination of Gaussian–Lorentzian shaped curves, centred on the identified peaks, were compared with the original spectra and showed good agreement.

1. Introduction

Ocean colour sensors mounted on satellites and aircraft have allowed the estimation of phytoplankton biomass using ratios of water-leaving radiance at different spectral bandwidths (see, e.g., Gordon *et al.* 1983). The launch of higher resolution sensors (e.g. Medium Resolution Imaging Spectrometer (MERIS)) will provide opportunities to gain more information about the light absorbing properties of phytoplankton. If major differences in taxonomic groups can be identified by their variation in light absorbing properties, these new sensors will provide exciting opportunities to differentiate between phytoplankton populations on a global scale. Although it is widely recognized that differentiation of mixtures of phytoplankton taxonomic groups may prove difficult, where monospecific algal blooms develop, high-resolution optics are considered a useful tool (Jeffrey 1997). Another approach

§To whom correspondence should be addressed.

International Journal of Remote Sensing
ISSN 0143-1161 print/ISSN 1366-5901 online
http://www.tandf.co.uk/journals

is to identify spectral peaks associated with particular pigments, or optical markers, of particular phytoplankton taxonomic groups (Barlow *et al.* 1993).

Since the absorption spectra of phytoplankton are complex due to the mixtures of pigments and associated proteins, it is difficult to identify these components by optical analysis. Some studies have focused on separating the absorption of chlorophyll-*a* from that of accessory pigments. Among these studies the derivative analysis of spectral curves has proven to be a powerful method (Bidigare *et al.* 1989). Derivative analysis is useful for resolving secondary peaks and shoulders produced by pigments present in the algae within the overlapping absorption regions (Butler and Hopkins 1970). Absorption maxima found using this method occur near or at the correct wavelength position, where absorption peaks may be attributed to particular photosynthetic pigments.

Over the last 25 years there have been considerable efforts to identify the components of algal absorption using mathematical techniques. French *et al.* (1972) deconvolved red absorption spectra of chlorophyll-*a* in green plants, using a Gaussian curve-fitting approximation. Their results were in good agreement with the conclusions of both room-temperature first-derivative spectral analyses (Gulyayev and Litvin 1970) and low-temperature fourth-derivative spectroscopic analyses (Butler and Hopkins 1970). Hoepffner and Sathyendranath (1991) applied a Gaussian approach to decompose *in vivo* absorption spectra of different algal cultures.

Another approach utilizes one of the simplest theoretical models of absorption proposed by H. A. Lorentz. Near the beginning of the twentieth century Lorentz developed a classical theory of optical properties in which the electrons and ions of matter were treated as simple harmonic oscillators subject to the driving force of applied electromagnetic fields (Bohren and Huffman 1983). The Lorentz model has been applied in molecular biophysics to explain the electronic excitation energy travelling in a periodic structure; this is the so-called exciton theory (Dexter and Knox 1965). Pigment molecules provide excellent examples of the usefulness of the analysis of excitation interactions, particularly their observation in absorption spectra (Sauer 1975). Bricaud and Morel (1986) successfully applied the Lorentzian model to decompose the absorption spectrum of the alga *Platymonas suecica*.

However, when considering the shape of the absorption spectra it is necessary to take into account the distortion caused by the dispersive slit. When the bandwidth and/or the components' bands are of the same order as the slit width a distortion may occur. In this case it is difficult to determine the true band shapes from the observed ones. There are, however, two methods of tackling this problem. (1) When the true shape of the spectrum is unknown but the instrument distortion is analytically known or can be easily measured, a deconvolution can be applied using Fourier methods (Boldeskul *et al.* 1971). (2) When the true band shape and the slit function are known, the observed shape can be calculated by convolution. Thus, when the true band shape is known as a function of the band parameters (position, half-width and weight) the convoluted curve can be calculated and the parameters varied until a good fit between the convoluted function and the data is obtained. This approach is used in the present study.

For a modern monochromator, the slit function is very similar to a Gaussian, at least for small slit widths (Sundius 1973). Thus, if the true band shape can be approximated by a Lorentzian shape, the observed profile will be the convolution of a Gaussian and a Lorentzian. This type of convolution has long been used in astrophysical spectroscopy (Mitchell and Zemansky 1934) but, to our knowledge,

there has been no attempt to combine Lorentzian and Gaussian models for the decomposition of absorption spectra of different alga. This approach appears to be comprehensive as the theoretical Lorentzian absorption spectral shape is smeared with a Gaussian deconvolution, which is caused by the optical design of a spectrophotometer.

In this study the derivative method will be used to identify the major absorption peaks of algae. Firstly, theoretical spectra for a number of taxonomic groups will be constructed and the derivative method will be used to identify the peaks. If these peaks are identified as those of the individual pigments used to construct the model, the method can be explored further with monocultures and finally with natural populations. The absorption spectra of a number of algal cultures will then be analysed, using both *in vivo* samples and samples in which the pigments have been extracted from the cells using solvents. This will be followed by analysis of the absorption spectra from a number of natural populations. The peaks identified from the solvent-extracted and natural samples will be compared with those expected from the component pigments and those measured by High Performance Liquid Chromatography (HPLC). A comparison will be made between the measured spectra and simulated spectra, which are constructed from individual, pigment absorption spectra. Finally, a method to simulate absorbance spectra, using a combination of Gaussian/Lorentzian curves centred on the derived spectral peaks, will be used to maximize the fit of a modelled spectrum to a measured one.

2. Methodology

2.1. *Derivative analysis*

When attempting to analyse the absorption spectrum of phytoplankton it is necessary to detect and determine quantitatively the position and the intensity of a weak absorption band which may be overlaid or obscured by another absorption band. Derivative analysis aims to provide a mathematical basis for identifying the main bands, and hence the components, of the absorption spectrum. It provides information regarding the convexity and concavity of a given absorption curve, and is useful for separating the secondary absorption peaks and shoulders produced by algal pigments in regions of overlapping absorption.

The derivative of a curve is simply its slope at a given point. In calculus notation, the derivative of the spectral trace is $\mathrm{d}A/\mathrm{d}l$, where A is the absorbance and l is the wavelength. The derivative is thus a plot of the slope $\mathrm{d}A/\mathrm{d}l$ against l. However, if the differentiation interval is very small, then the difference between the successive values may be small compared with the random noise and a noisy derivative spectrum may be obtained. On the other hand, a larger differentiating interval will reduce the noise and maximize the signal, but sharp features may be lost. Butler and Hopkins (1970) found that the optimum differentiating interval depends on the level of noise in the data and the spectral bandwidth of the signal.

The derivative plot has some advantages over a direct record. For example, it indicates more precisely the centre of each absorption peak. Figures 1(*a*) and 1(*b*) show, respectively, a schematic diagram of the simulated Gaussian and Lorentzian absorbance curve and four derivatives ($\mathrm{d}^n A/\mathrm{d}l^n$ $n = 1,2,3,4$). At the centre of a peak the curve is horizontal, hence $\mathrm{d}A/\mathrm{d}l$ shows an inflection point parallel to the axis l. These inflection points indicate the presence of either a maximum or a minimum in the curve (see the first derivative in both figures). The use of derivative analysis to identify small changes in the slope of spectra can be observed in these figures, which

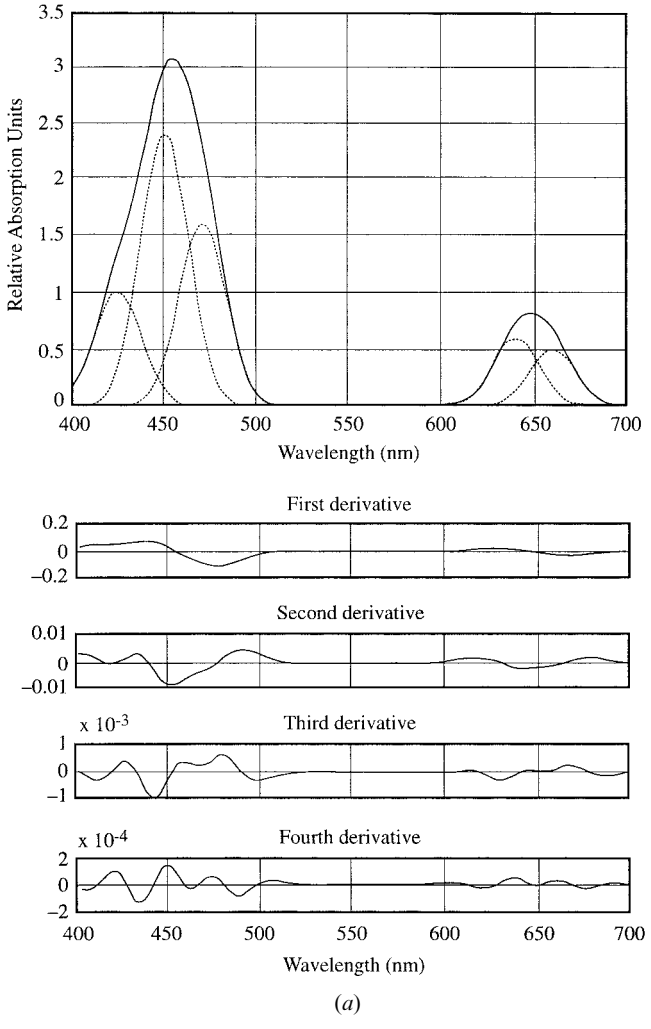

(*a*)

Figure 1. (*a*) Simulated absorption spectrum using five Gaussian curves and a step-by-step derivative process. (*b*) Simulated absorption spectrum using five Lorentzian curves and a step-by-step derivative process.

show the sum of five simulated absorption curves. In figure 1(*a*) the individual curves are Gaussian-shaped whilst in figure 1(*b*) they are Lorentzian-shaped. These curves have their central wavelengths at 425, 450, 470, 640 and 660 nm and intensities of 1, 2.4, 1.6, 0.6 and 0.5 relative units, respectively. The half-width is 30 nm for all the curves, in both cases. These values are rather arbitrary but simply aim to provide a typical simulated absorption curve.

In order to determine whether the inflection points represent a minimum or a maximum, the second derivative is calculated. The maxima are found by looking at the negative minima in the second-derivative spectrum. It is, however, important to note that not all the peaks have been resolved with the second derivative, particularly in the case of the Gaussian curves (figure 1(*a*)). Since there are still unresolved peaks, it is necessary to continue with the derivative analysis. The third derivative provides similar information to that of the first derivative and, by looking at the inflection

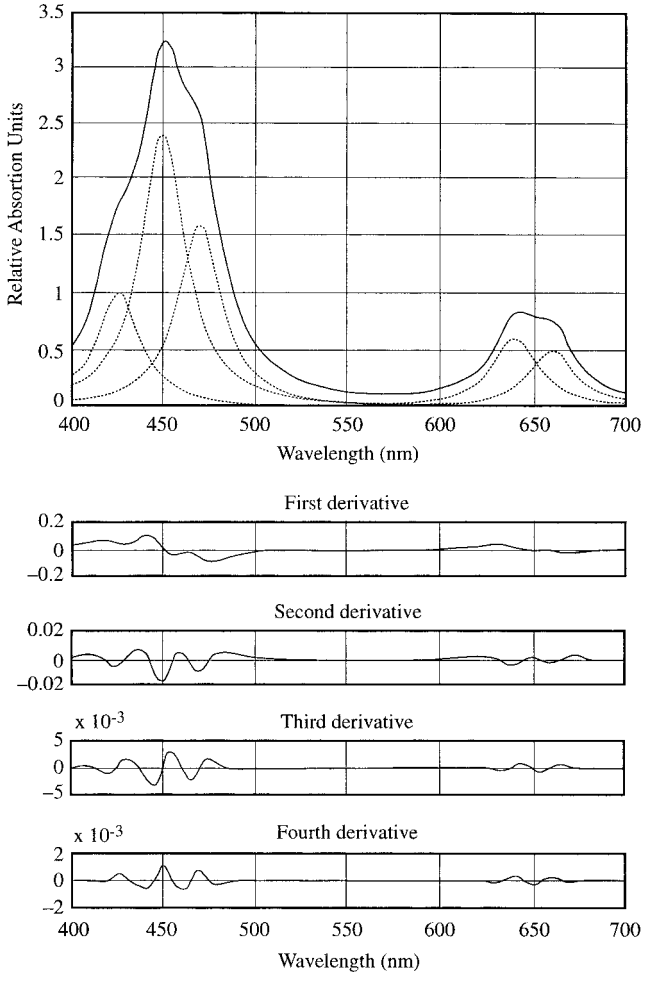

(*b*)

points on this curve, a new set of maxima and minima becomes apparent. The third-derivative curve is almost an inverse image of the first derivative, but has the advantage of enhancing subtle features. This is evident when comparing both curves at every bandwidth marked in the grid. With this information, it becomes apparent that the positive maxima of the fourth derivative correspond to the inflection points of the third derivative. Again, the fourth-derivative curve is almost the inverse of the second-derivative curve, except that the former shows new features which were unresolved in the latter. In the case of the Lorentzian curves, the second derivative was sufficient to resolve the peaks of the five component spectral curves. This can be observed in figure 1(*b*). However, to resolve all the Gaussian peaks it was necessary to continue up to the fourth derivative.

2.2. *Gaussian–Lorentzian deconvolution*

To understand the absorption characteristics of phytoplankton it is important to analyse the physical and instrumental mechanisms involved in the process. The shape of absorption spectra is conformed largely by both factors. These factors can be

represented by well known mathematical functions. The two most commonly observed shapes are the Lorentzian and Gaussian. These curves are analytically represented by the following expressions.

Gaussian function

$$Y = Y_0 \exp\left[- \ln 2 \left(\frac{2(X - X_0)}{\Delta X_{1/2}} \right) \right]^2 \quad (1)$$

Lorentzian function

$$Y = Y_0 \left[1 + \left(\frac{2(X - X_0)}{\Delta X_{1/2}} \right)^2 \right]^{-1} \quad (2)$$

where Y_0 represents the band height, X represents the abscissa coordinate of the peak X_0 and $\Delta X_{1/2}$ is the bandwidth at half-height.

Among other physical reasons, electrons and ions of interacting molecules can theoretically be regarded as simple harmonic oscillations in an electromagnetic field, resulting in a Lorentzian shape. However, when measured by an optical spectrophotometer the signal is transformed into a Gaussian curve. Thus, a combination of both types of curve provides a realistic approach for analysis of absorption spectra. Thus, in any attempt to reconstruct the absorption coefficient $a_{ph}(\lambda)$ of phytoplankton, all of these factors have to be taken into account.

2.3. *Physical factors of spectral absorption lines broadening*

Molecules have three main types of energy. A molecule may possess rotational energy due to a bodily rotation about its centre of gravity; it may have vibrational energy due to the periodic displacements of its atoms from their equilibrium position; and it may have electronic energy since the electrons associated with each atom or bond are in constant motion (Rees 1990).

The absorption spectrum of any pigment is a signature of the energy levels most effectively absorbed, and reflects the electronic state characteristics of the nuclear structure of the molecule (Sauer 1975). The final spectrum, however, is not a simple one—it can appear broadened by three main effects: Doppler broadening; Heisenberg's uncertainty principle; collision broadening (Schanda 1986).

2.3.1. *Doppler broadening*

Absorption spectra can have a Gaussian shape caused by Doppler shift effects, which makes the absorption spectral lines broader than might be expected (Schanda 1986). It has been found that in the visible region at room temperature the Doppler (Gaussian) width is comparable to the resolution limit of a large grating spectrophotometer, which may account for up to a maximum of 1 nm (Thorne 1974).

2.3.2. *Natural line shape (Heisenberg's uncertainty principle)*

The energy–time uncertainty relation shows that a state with a finite lifetime does not have a precisely defined energy; rather its energy has a spread or uncertainty, which increases with decreasing lifetime. Apart from the ground state, all other energy states show spontaneous emission. Thus, an excited state does not show a sharply defined energy. The line shape of the energy distribution is a typical example of a Lorentzian curve. The classical natural width in the visible (400–700 nm) has been estimated as 1.6×10^{-5} nm, constant for all wavelengths (Thorne 1974). Thus, the contribution of this mechanism to band broadening is small enough to be detected by optical instruments.

2.3.3. *Collision broadening*

Molecules of condensed matter (liquids and gases) are in continuous motion and frequently collide. These collisions produce some deformation of the particles and perturb the energies of at least the outer electrons in each particle. This fact accounts for the width of visible spectral lines, since these deal largely with transitions between outer electronic shells. Because of these collisions, the temperature of the medium may increase. So, an equilibrium must be reached between the thermal energy and the electrical energy of the molecular oscillations. This fact indicates that the spectral properties of the absorption lines reflect the kinetic temperature of the medium. It is not straightforward to give a typical value of the broadening created by this mechanism as many physical assumptions are involved in the process. However, the contribution due to this broadening effect may be from 2 to 10 nm, mainly depending on the type of molecular collision involved. Collision broadening is known to adopt a Lorentzian shape (Thorne 1974).

2.4. *Instrumental factors for spectral absorption line broadening*

A number of studies have shown that in analysing the shape of absorption spectra it is necessary to consider the distortion caused by the dispersive slit of a spectrophotometer. Basically, a double beam UV–visible spectrophotometer consists of a source of light, an optical arrangement and a photosensor.

The physical width of the beam falling on the photosensor can be limited by the provision of an exit slit just in front of the detector entrance. However, since it is impossible to make either of the slits infinitely narrow, a range of wavelengths, rather than a single one, falls on the photosensor. This results in a broadening of the absorbance peaks of the substance. It has been found that this effect smears the signal into a Gaussian shape. Banwell (1972) provides a detailed description of this process.

The physical and instrumental factors discussed above confer the shape of Gaussian–Lorentzian curves to the absorption spectra of pigments. The convolution of these mathematical curves is known as the Voigt function.

2.5. *Voigt profile of the absorption coefficient of phytoplankton*

There are two important consequences when considering the broadening effects and the pigment composition expression. Firstly, the absorption coefficient of each pigment can now be estimated by decomposition of $a_{\mathrm{ph}}(\lambda)$ into several Gaussian–Lorentzian bands simulating the absorption properties of these pigments. This result means that the absorption coefficient of phytoplankton can be expressed as:

$$a_{\mathrm{ph}}(\lambda) = \sum_{i=1}^{n} C_i(\lambda_{\mathrm{m}\,i}) \{\mathrm{a}_i^* G + b_i^* L\} \tag{3}$$

where

$$G = \exp\left(\frac{(\lambda - \lambda_{\mathrm{m}\,i})^2}{w_i}\right) \tag{4}$$

is the Gaussian contribution to the phytoplankton absorption spectra.

$$L = \left[1 + 4\left(\frac{\lambda - \lambda_{\mathrm{m}\,i}}{w_i}\right)\right]^{-1} \tag{5}$$

is the Lorentzian contribution to the phytoplankton absorption spectra; $\lambda_{m\,i}$ is the position of maximum absorption for the ith Gaussian–Lorentzian contribution; w_i determines the width of the peak; a_i^* is the mean specific absorption coefficient for the ith Gaussian absorption band at $\lambda^*_{m\,i}$, b_i^* is the mean specific absorption coefficient for the ith Lorentzian absorption band at $\lambda_{m\,i}$; and C_i is the concentration of the pigment responsible for the ith absorption band. This expression contains the physical and instrumental elements for the spectral reconstruction of the absorption coefficient of phytoplankton $a_{ph}(\lambda)$ through a Gaussian–Lorentzian deconvolution. Consequently, the original or the reconstructed Gaussian–Lorentzian absorption spectra of phytoplankton can be used indistinctly, but the latter approach has the advantage of being suitable for a mathematical treatment.

The second consequence of spectral broadening is that absorption spectra of biological material becomes a rather complicated mixture of absorption bands that very often are difficult to resolve into their individual components. Improvements in resolving power can be achieved not only by using better electro-optical designs, which can be very expensive, but also by applying mathematical techniques to the experimental data. In this respect, Butler and Hopkins (1970) have shown that derivative analysis is useful for resolving overlapping absorption regions. The next section shows how, through this method, the position of the maximum absorption peak $\lambda_{m\,i}$ can be objectively located.

2.6. *Voigt curves fitting*

In order to determine the optimum combination of Voigt curves, the curve fitting program RESOL, initially described by French *et al.* (1969), was slightly updated and adapted to the requirements of this study. The program requires information about wavelength peaks, heights and half-widths. The first two parameters were provided by derivative analysis of the absorption spectra of the algae; the third was estimated based on a literature review (French *et al.* 1972, Hoepffner and Sathyendranath 1991). The procedure was applied to the absorption spectra of acetone-extracted and *in vivo* samples of phytoplankton, and also to the natural populations.

The input specifications for each absorption spectrum were: (a) both Gaussian and Lorentzian shapes for each curve-fitting analysis; (b) selected half-widths; (c) no weighting of the data (i.e. the program was allowed to work out the best combination of weights); (d) a maximum of 20 iterations; (e) band centres (derivative analysis) and hald-bandwidth changes of no more than 1 nm per iteration.

The program then optimized these parameters in each band to provide the best fit with the absorbency curve. Because all parameters are adjusted for each iteration the convergence was rapid. At the end the program gave the values of four parameters: the central peak, the Gaussian weight, the Lorentzian weight and the half-width.

Section 3 shows how this method was used to locate the position of the maximum absorption peak $l_{m\,i}$.

3. Results

3.1. *Modelled absorption spectra*

The derivative method was applied to two modelled absorption spectra of diatoms and green algae, these containing phytoplankton with different pigment assemblages and concentrations and, hence, different optical characteristics.

The spectral curves were constructed in the following way. Initially, the individual

pigment spectra for each pigment (taken from Prézelin and Bóczar (1986), Kirk (1983) and Jeffrey (1980)) were digitized for computer handling and then normalized for standardization purposes. These spectra were then multiplied by a proportionality factor and each of the component pigments summed to obtaining the absorption spectra. The proportions of the different pigments present in each alga were taken from the works of Kirk (1983) and Jeffrey (1980). Peak positions for the most representative pigments were compared with those reported in the literature (e.g. Bidigare *et al.* 1989, Prézelin and Bóczar 1986, Hoepffner and Sathyendranath 1991) and are summarized in table 1.

3.1.1. *Diatoms*

This kind of algae usually has a yellow–brown colouration produced by the masking effects of fucoxanthin pigments over the chlorophylls (Boney 1976). These algae contain photosynthetic pigments of chlorophyll-*a*, chlorophyll-c_1, chlorophyll-c_2, fucoxanthin and a low amount of β-carotene (Prézelin and Bóczar 1986).

The proportion of chlorophyll-*c* is, on a molar basis, about the same as chlorophyll-*b* has in green algae and higher plants (Kirk 1983). The mean value of the molar ratio of chlorophyll-*a* to chlorophyll-*c* is about three (considering $c = c_1 + c_2$). Jeffrey (1976) stated that the relative amount of chlorophyll-c_1 to c_2 has been found to be one in most cases. Gugliemelli *et al.* (1981) found a molar ratio of carotenoid to chlorophyll-$(a + c)$ in the diatom *Phaeodactylum* of about 1:0.5. Here, carotenoid includes both fucoxanthin and β-carotene in the proportion 1:1. The relative proportions of chlorophyll-*a*, chlorophyll-c_1, chlorophyll-c_2, fucoxanthin and β-carotene were used for constructing the absorption spectrum for a diatom (D) as follows:

$$D = 0.5[3\,\text{Chl-}a + \text{Chl-}(c_1 + c_2)] + (\text{fucoxanthin} + \beta\text{-carotene}) \tag{6}$$

3.1.2. *Green algae*

These phytoplankton contain pigmentation closely resembling the chlorophyll-*a*–chlorophyll-*b*–carotenoid system characteristic of higher plants (Prézelin and Bóczar 1986). In higher plants and in fresh water green algae, the molar ratio of chlorophyll-*a* to chlorophyll-*b* is about 3:1 (Kirk 1983). However, several marine species of green algae are characterized by low chlorophyll-*a*/*b* ratios, lying in the range 1.0 to 2.3 (Yokohama and Misonou 1980). Kirk (1983) reports that in higher plants and green algae the molar ratio of carotenoids to chlorophyll-$(a + b)$ is about 1:3. Although not the predominant carotenoid, β-carotene pigment is present in almost all algal groups (Kirk and Tilney-Bassett 1978); it was therefore chosen as

Table 1. Position of peaks of pigments and those found for the modelled theoretical curves through the derivative analysis. Shoulders are marked with the symbol (~).

Case/pigment	Peak position (nm)										
Diatom	431	460	487		531		577	617	634		661
Green algae	430	457	488	512	533	562	579	612		643	662
Chlorophyll-*a*	430							~610			660
Chlorophyll-*b*	~430	453								645	
Chlorophyll-c_1		446					580		628		
Chlorophyll-c_2		449					580		628		
β-carotene		450	480								
Fucoxanthin		460	480								

the representative carotenoid pigment used in this test. These observations have been used to construct the absorption spectrum of green algae (*GA*) using the following relationship:

$$GA = 3(1.6\,\text{Chl-}a + \text{Chl-}b) + \beta\text{-carotene} \quad (7)$$

the value of 1.6 corresponds to the mean of the Chl-*a*/Chl-*b* ratio for marine species.

3.2. *Derivative analysis of the modelled absorption spectra*

The derivative method was applied to both constructed theoretical curves (equations (6) and (7)).

3.2.1. *Diatoms*

The peaks found through use of the fourth-derivative algorithm were located at the following wavelengths: **431**, **460**, **487**, 531, 577, **617**, **634** and **661** nm. Those peaks that are attributable to light absorbing pigments are shown in bold. A comparison of these values with those in table 1 shows that the peaks located at 431 and 661 nm approximately coincide with the expected peaks of chlorophyll-*a*. The peak at 617 nm is probably due to the presence of chlorophyll-*a*, but it has been slightly reinforced by the presence of both types of chlorophyll-*c* pigments. The peak appearing at 460 nm may also be due to the mixture of both types of chlorophyll-*c*, while the peak located at 634 nm is probably entirely caused by the presence of chlorophyll-c_2. Finally, the peak at 487 nm is produced by a combination of fucoxanthin and β-carotene.

Due to the fact that both types of chlorophyll-*c* overlap in the blue region, with chlorophyll-c_1 completely masking chlorophyll-c_2, the peaks are unresolved. Likewise, fucoxanthin and β-carotene have either very close absorption peaks or peaks at the same wavelengths; this results in a reinforced absorption peak rather than in separated peaks. Figure 2(*a*) shows the diatom absorption spectra with its component pigments (upper panel) and the fourth-derivative curve (lower panel).

3.2.2. *Green algae*

Absorption peaks for the theoretical curve of green algae were found at the following wavelengths: **430**, **457**, **488**, 512, 533, 562, 579, **612**, **643** and **662** nm. It should be noted that the peaks appearing in the green region (500–600 nm) are small compared to those located in the blue and red regions (bold numbers), which have a clear biological significance. A comparison of these values with those in table 1 shows that the peaks located at 430, 612 and 662 nm coincide with the expected peaks of chlorophyll-*a*. Peaks located at 457 and 643 nm may be attributed to chlorophyll-*b*. The β-carotene pigment matches the peak at 488 nm.

It should be noted that some peaks may appear slightly shifted from their expected positions, especially when two absorption peaks are very close. During summation the curves combine and the peaks are shifted to one side or the other of the original curve. In these cases the resultant absorption peak would appear shifted

Figure 2. (*a*) Top, theoretical absorption spectrum of a diatom (——) based upon the relative proportions of chlorophyll-*a* (-·-); chlorophyll-$c_1 + c_2$ (◆); β-carotene (:) and fucoxanthin (- -) (see text). Bottom, peaks determined by the fourth-derivative analysis. (*b*) Top, theoretical absorption spectrum of green algae (——) based upon the relative proportions of chlorophyll-*a* (-·-); chlorophyll-*b* (:); and β-carotene (- -) (see text). Bottom, peaks determined by the fourth-derivative analysis.

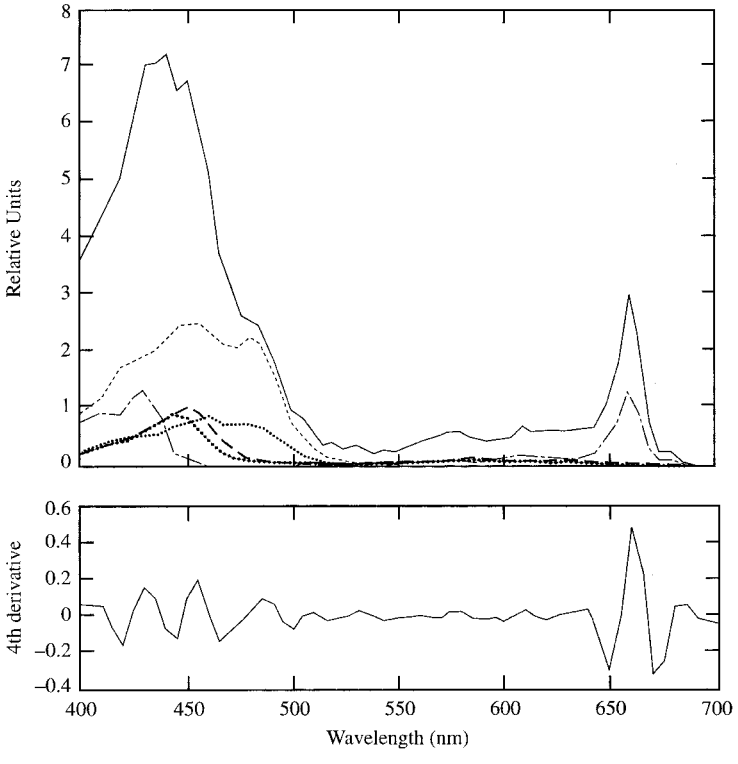
Relative Units
4th derivative
Wavelength (nm)

(*a*)

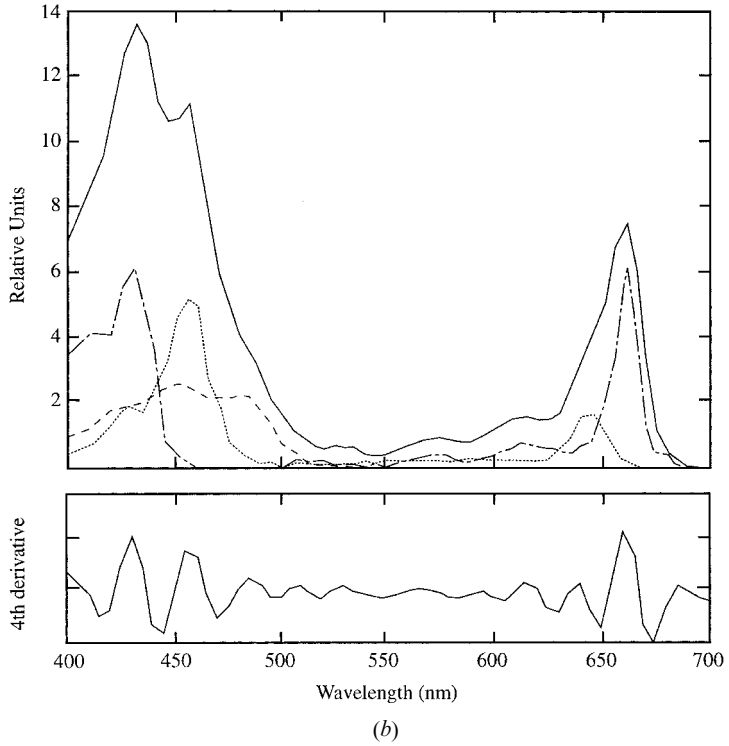
Relative Units
4th derivative
Wavelength (nm)

(*b*)

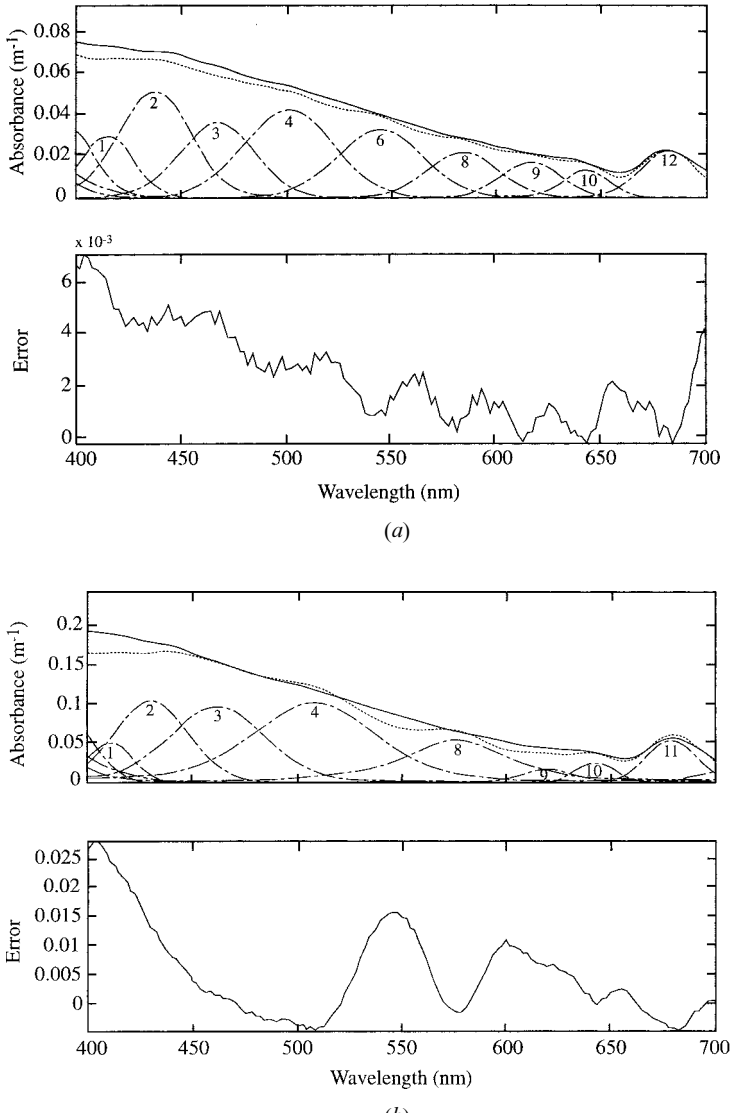

Figure 3. Absorption spectrum of *in vivo* monocultures of (*a*) *Phaeodactylum* and (*b*) *Tetraselmis*: full curves, reconstructed absorption curve; dotted curve, using a Gaussian–Lorentzian convolution (see text). The component curves, calculated by the convolution and the Gaussian/Lorentzian shapes are also shown. The bottom panel shows the magnitude of error between the two curves.

towards the major pigment, according to the magnitude of the absorbing pigment. For example, two chlorophyll-*a* peaks should exist at the blue region of the spectrum, but as both chlorophyll-*b* and β-carotene spectra have a monotonic and ascendant response in the blue, they compensate for the chlorophyll-*a* depression between the peaks at 410 and 430 nm. Figure 2(*b*) shows the original green algae spectrum with its component pigments (upper panel) and the fourth-derivative curve (lower panel).

These results show that by reconstrucing spectra from component pigments, derivative analysis can be used to determine original spectrum peaks.

3.3. *Cultured samples*

The next stage was to determine the major spectral peaks in a number of algal cultures and to consider the pigments these represent, particularly considering the presence of biomarkers for particular taxonomic groups. Mantoura and Llewellyn (1983) have developed methods for identifying and determining the concentration of the major light absorbing pigments using HPLC. Following this method a number of algal groups were analysed in order to determine their pigment characterization (table 2). This shows, for example, zeaxanthin is a biomarker for Synechococcus, while peridinin is a biomarker for dinoflagellates. Similarly, diatoms do not contain peridinin and zeaxanthin, but they do contain fucoxanthin.

There are, however, a number of problems with this approach. The HPLC technique requires that the pigments are isolated from the cell and, for the majority of pigments, this is most effective when solvents are used. The absorption properties of intact phytoplankton differ from the extracted samples due to the fact that pigments are bound with protein complexes. Additionally the package effect may produce different absorption characteristics in whole cells, and this is particularly important in larger cells (Morel and Bricaud 1981). Therefore, comparison of spectral peaks with HPLC derived pigments can only be carried out effectively for absorption spectra of solvent-extracted phytoplankton. Comparisons were made for *in vivo* monocultures and natural populations, with consideration given to spectral shifts.

3.4. *Spectrophotometric measurements on* in vivo *samples*

Species in culture included a diatom (*Phaeodactylum tricornotum*) and a chlorophyte (*Tetraselmis suecica*), selected for their different pigment composition and therefore different colour. Values of the absorption coefficient of phytoplankton were taken from a direct measurement of whole suspended particles according to the technique presented by Lewis *et al.* (1985) and Sathyendranath *et al.* (1987). The samples of water containing intact phytoplankton cells were located just at the entrance of the spectrophotometer's photomultiplier in order to increase the scattering reception angle. Bricaud *et al.* (1983), using angular scattering fucntions representative of phytoplankton, calculated that in this way more than 99.5% of the scattered light can be captured. The samples were prepared by obtaining three 5 ml

Table 2. Pigments detected by HPLC and their respective concentrations ($\mu g l^{-1}$) (after Mantoura and Llewelyn (1983)).

Pigment	*Phaeodactylum tricornotum*	*Rhizosolenia delicatula*	*Synechococcus* sp.	*Amphidinium carterae*
Chl-c_3	0.40	3086.46	183.92	0.30
Chl-c_1 + -c_2	2637.24	2787.19		1191.40
Fucoxanthin	3850.72	3921.25	480.84	
Peridinin				926.84
Diadinoxanthin	2199.85	1421.06		5167.24
Chl-*a*	3119.11	969.68	1451.90	7095.96
β-carotene	167.39	92.86	1569.99	583.66
Zeaxanthin			1080.18	

units from an aseptic 25 ml sample of each alga. Absorption spectra measurements were calibrated by placing two samples of filtered seawater at the entrance of the photomultiplier. The response was a flat line that was then zeroed to yield a background correction factor. This process was repeated before each new measurement. The absorption spectrum of each unit was measured from 350 to 750 nm, using filtered seawater as a blank, in a Hitachi Model U-2000 double beam spectrophotometer with a spectral resolution of 2 nm. The path length of the sample cells was 1 cm. The mean of these spectra was taken as representative with a standard error of less than 2.5% between replicates.

3.5. *Derivative analysis of measured absorption spectra of algal cultures*

The derivative method was applied to the absorption spectra of the diatom *Phaeodactylum tricornotum* and the chlorophyte *Tetraselmis suecica* and the results are shown in tables and figures 3a and 3b respectively. The major light absorbing pigments, namely chlorophyll-*a* and carotenoids, are the cause of these peaks. Since chlorophyll-*a* is common to both kinds of algae, it is discussed separately; the other pigments are discussed as a different group.

Table 3a. Absorption peaks (nm) for *in vivo* cultures of *Phaeodactylum tricornotum* from the fourth-derivative method and curve-fitting procedure, including proportions of Gaussian and Lorentzian weights.

No.	Original peak (nm)	Adjusted peak (nm)	Gaussian weight	Lorentzian weight
1	418	414.72	0.5214	0.0000
2	442	437.13	0.1587	0.0000
3	466	466.88	0.4666	0.0096
4	500	500.79	0.3456	0.0128
5				
6	544	544.31	0.2151	0.0000
7				
8	586	584.11	0.3158	0.0000
9	616	616.54	0.2623	0.0062
10	638	642.62	0.2101	0.0193
11	680	681.48	0.3455	0.1990

Table 3b. Absorption peaks for *in vivo* cultures of *Tetraselmis suecica* from the fourth-derivative method and curve-fitting procedure, including proportions of Gaussian and Lorentzian weights.

No.	Original peak (nm)	Adjusted peak (nm)	Gaussian weight	Lorentzian weight
1	414	411.40	0.4741	0.0000
2	440	430.50	0.1583	0.0000
3	466	461.93	0.2885	0.0200
4	500	508.08	0.1465	0.0132
8	590	575.99	0.1956	0.0011
9	620	620.17	0.1737	0.0000
10	640	643.12	0.1112	0.0142
11	680	678.80	0.2845	0.0010

3.5.1. *Chlorophyll*-a

Consideration of the other results suggests that absorption peaks 1, 2, 9 and 11, with their maxima at 415–425, 440–455, 620 and 675 nm respectively, correspond to *in vivo* absorption by chlorophyll-*a*. Goedheer (1970) observed that the *in vivo* absorption spectra of the brown algae *Laminaria digitata* had chlorophyll-*a* peaks at 418, 437, 618 and 673 nm. Prézelin (1980) found absorption peaks of *Glenodinium* sp. at 419, 437, 618 and 675 nm. More recently, Hoepffner and Sathyendranath (1991) reported averaged values of chlorophyll-*a* absorption peaks of three different groups of algae, located at 412, 435, 623 and 675 nm. These values are similar to those found here.

3.5.2. *Carotenoids*

In relation to carotenoid-like pigments, the range of absorption maxima is wider than that of chlorophyll-*a*. However, similar results to those found here have been reported. Mann and Myers (1968) assigned the range 425–530 nm to carotenoids, with the range 460–530 nm due to fucoxanthin and that of 425–500 nm due to β-carotene. Similarly, Bidigare *et al.* (1989) located the fucoxanthin absorption range at between 521 and 531 nm. Hoepffner and Sathyendranath (1991) concluded that the peaks found at 489 and 536 nm may correspond to a mixture of carotenes and xanthophylls rather than to the separate groups. Xanthophylls differ from carotenes by the presence of oxygenated groups in their molecules, but this alone is not sufficient to distinguish them by their spectra.

Peak 6, located between 545–555 nm, may also be attributed to fucoxanthin. In support of this, Goedheer (1970) detected fucoxanthin in the *in vivo* absorption spectrum of *Laminaria digitata* in the interval 530–545 nm. Finally, peak 8, located at 590–600 nm, may be attributed to chlorophylls. For example, a small feature at 585 nm due to chlorophyll-*c* was observed in the *in vivo* absorption spectrum of *Laminaria digitata* (Goedheer 1970). However, the same feature was observed in some absorption spectrum of chlorophyll-*a*–chlorophyll-*c*–protein complexes (Prézelin and Bóczar 1986).

There are a number of peaks that are characteristic of pigments only found in some of the algae. In the case of *Phaeodactylum tricornotum*, apart from chlorophyll-*a* peaks (415, 440, 620 and 675 nm), there are two peaks (470, 640 nm) caused by the presence of chlorophyll-($c_1 + c_2$) and, in the green region, four absorption peaks (505, 530, 545 and 590 nm) due to carotenoid-like pigments. In relation to both types of chlorophyll-*c*, several authors have reported similar results. For instance, Hoepffner and Sathyendranath (1991), averaging over a number of diatoms, found two *in vivo* absorption peaks of chlorophyll-*c* at 460 and 642 nm; Bidigare *et al.* (1989) also reported two absorption peaks of chlorophyll-*c* located at 467 and 630 nm. Similarly, Mann and Myers (1968) found absorption maxima at 460 and 640 nm.

In the case of *Tetraselmis suecica*, peaks attributable to chlorophyll-*a* were located at 425, 455, 620 and 675 nm. Chlorophyll-*b* peaks appeared at 480 and 640 nm. Carotenoid–xanthophyll pigment peaks were found in the green region ranging from 505 to 575 nm. The peak located at 600 nm may be attributed to the influence of the chlorophyll-*a*–chlorophyll-*b* complex. Chlorophyll-*b* absorption peaks have been found in a range of positions in the blue region of green algae spectra. For instance, Gulyayev and Litvin (1970) assumed that peaks appearing at 442–446, 470–474 and 641–650 nm are due to this pigment. Bidigare *et al.* (1989) found absorption peaks at 483 and 650 nm. Hoepffner and Sathyendranath (1991) interpreted that, on

average, the absorption peaks at 463 and 654 nm are due to chlorophyll-*b*. Jeffrey (1980) found that in the *in vivo* spectra of three marine species of green algae, chlorophyll-*b* contributes with a shoulder, sometimes a peak, at about 650 nm and adds to the strong blue light absorption around 440–460 nm.

3.6. *Spectrophotometric measurements on acetone-extracted samples*

In the laboratory, two aseptic 5 ml samples of the diatom *Phaeodactylum tricornotum* and the blue–green alga *Synechococcus* sp. were filtered through a 47 mm glass fibre filter (Whatman GF/F) using a Millipore vacuum pump. The filters were folded in half, with the algal material inside, placed in a plastic bag, wrapped in aluminium foil, labelled and stored at -20°C. The filters were subsequently manually ground using a glass rod and then homogenized with a motorized homogenizer (Gallenkamp) in 6 ml of 90% of acetone. Homogenization continued until the filters were well ground. The homogenized algal material was placed in a parafilm-covered tube and centrifuged at 3000 rpm for ten minutes (Mistral MSE 2000). A small amount of the extract was then used for HPLC pigment analysis and a 5 ml sample for absorption measurements using the spectrophotometer. Absorption spectra measurements were calibrated and corrected for background noise by placing two samples of acetone in the cuvettes and measuring the spectrum. The process was repeated before each measurement. Absorption spectra were recorded from 350 to 750 nm in triplicate using 90% acetone as a blank. The path length of the sample cells was 1 cm. The mean spectrum of each sample was taken as representative. The standard error between replicates was less than 1%. Samples were measured using a Hitachi Model U-2000 double beam spectrophotometer with a spectral resolution of 2 nm and an instrumental error of ± 1 nm.

3.7. *Derivative analysis of acetone-extracted cultured samples*

Derivative analysis was performed and the results are shown in tables 4a and 4b. Peaks were found both in the blue and in the red regions, with minor peaks located in the green part of the spectrum. More specifically for the diatom *Phaeodactylum* (table 4a) peaks 1, 2, 6 and 7 can be attributed to chlorophyll-*a*, while peak 3 can be attributed to chlorophyll-*c*, and peaks 4 to 5 to fucoxanthin and to carotenoid complexes respectively. For the green alga *Synechococcus* (table 4b) peaks 1, 2, 6 and 7 are attributable to chlorophyll-*a*, peak 3 to β-carotene, 5 to fucoxanthin and 4 to carotenoid complexes. These peaks were compared with the results from HPLC analysis, which showed the presence of a number of pigments and their concentrations (table 4c). Fucoxanthin was found in *Phaeodactylum*, a biomarker for diatoms. Zeaxanthin, a biomarker for *Synechococcus*, was present in the blue green alga. Since *Synechococcus*' biliproteins are water soluble they were not considered in this analysis.

Figures 4(*a*) and 4(*c*) show the absorption of *Phaeodactylum tricornotum* and *Synechococcus* sp respectively. Once the pigments had been identified, the individual absorption spectra were combined to construct theoretical absorption spectra for each alga. However, since the pigments were extracted using a number of different solvents (which maximized the efficiency of extraction) different absorption peak positions and magnitudes are expected. Bearing this in mind, the spectra were reconstructed following the same procedure as for the theoretical spectra of diatoms and green algae. Thus, since the component pigments had been isolated using different solvents, a normalization procedure was carried out to avoid magnitude problems. A normalized value of one was given to the concentration of the major

Table 4a. Absorption peaks for solvent-extracted cultures of *Phaeodactylum tricornotum* from fourth-derivative method and the curve-fitting procedure, including proportions of Gaussian and Lorentzian weights.

No.	Original peak (nm)	Adjusted peak (nm)	Gaussian weight	Lorentzian weight
1	408	407.00	0.1578	0.000
2	434	434.12	0.3391	0.000
3	480	479.00	0.1605	0.000
4	538	537.00	0.0151	0.0005
5	578	579.00	0.0177	0.0001
6	622	623.00	0.0304	0.0005
7	662	663.00	0.1094	0.0036

Table 4b. Absorption peaks for solvent-extracted cultures of *Synechococcus* sp. from the fourth-derivative method and curve-fitting procedure, including proportions of Gaussian and Lorentzian weights.

No.	Original peak (nm)	Adjusted peak (nm)	Gaussian weight	Lorentzian weight
1	408	407.00	0.0001	0.0000
2	430	429.00	0.0700	0.0000
3	458	457.00	0.0437	0.0000
4	484	485.00	0.0300	0.0000
5	542	541.00	0.0065	0.0000
6	576	576.41	0.0022	0.0000
7	616	615.00	0.0076	0.0000
8	662	661.00	0.0380	0.0000

Table 4c. Pigment analysis (HPLC) showing pigments, their concentration in different algal groups and their retention times.

Pigment	Concentration ($\mu g l^{-1}$)	Retention time (min)
Phaeodactylum tricornotum		
Chlorophyll-c_3	30.20	03.73
Chlorophyll-$c_1 + c_2$	84.96	05.75
Fucoxanthin	328.31	09.90
Diadinoxanthin	107.21	10.81
Chlorophyll-*a*	794.20	13.06
β-carotene	8.82	14.73
Synechococcus sp.		
Chlorophyll-c_3	6.34	03.12
Fucoxanthin	41.00	09.87
Zeaxanthin	51.15	10.24

pigment. Then, based on that, a weighting factor was calculated for the remaining component pigments as the relative proportion in relation to the norm. Finally, a weighted sum according to the relative concentration of the pigments was the basis for plotting a reconstructed absorption curve. The reconstructed spectra of *Phaeodactylum tricornotum* and *Synechococcus* sp. are shown in figures 4(*b*) and 4(*d*) respectively, along with the original measured spectra and the spectra of the component pigments.

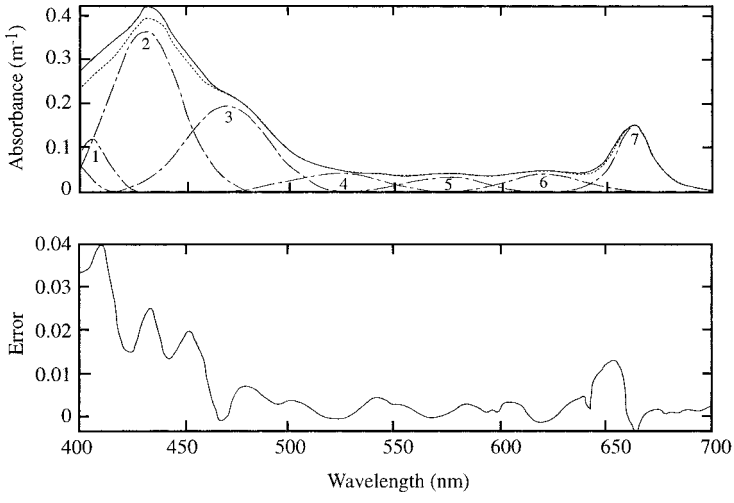

(*a*)

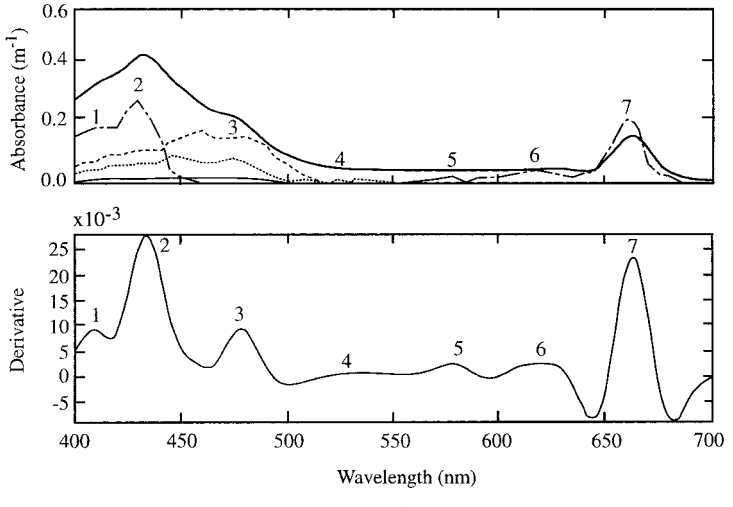

(*b*)

Figure 4. Absorption spectrum of solvent-extracted pigments of: (*a*) *Phaeodactylum*—this includes the reconstructed spectrum (dotted curve) by the Gaussian–Lorentzian convolution; the bottom panel shows the magnitude of the error between the two curves; (*b*) the measured absorption spectrum and the reconstructed spectrum of *Phaeodactylum* calculated by normalizing the pigment spectra; (*c*) *Synechococcus*—this includes the reconstructed spectrum (dotted curve) by a Gaussian–Lorentzian convolution; the bottom panel shows the magnitude of the error between the two curves; (*d*) the measured absorption and the reconstructed spectrum of *Synechococcus* calculated by normalizing the pigment spectra.

3.8. *Natural populations*

Natural populations were collected over several days during the early summer of 1995 at a site 12 km off the Plymouth coast (50° 10′ N, 4° 10′ W). The examples presented here were collected on 9 May, when two litres of seawater samples were collected onboard the research vessel *Squilla*. The samples were later analysed at the

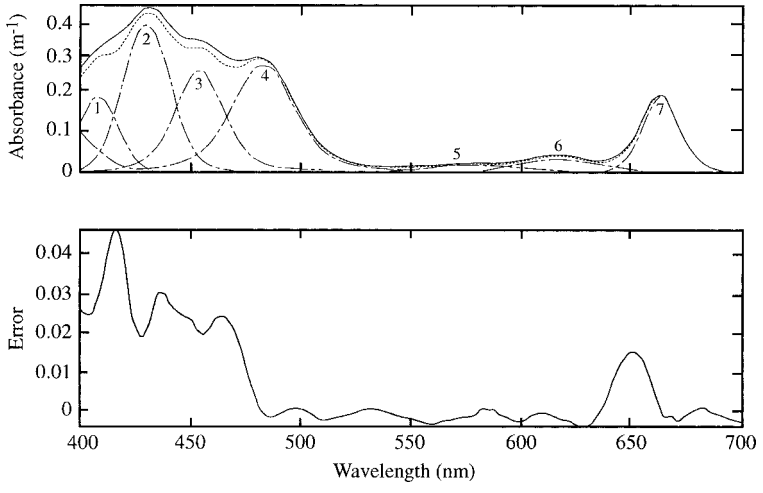

(*c*)

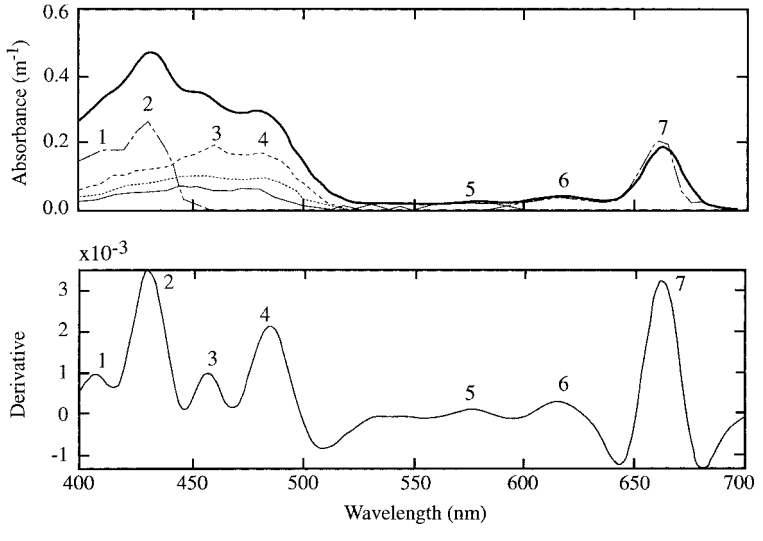

(*d*)

Plymouth Marine Laboratory (PML). Absorption spectra collected in the field were measured at PML using a double beam Perkin-Elmer lambda 2 spectrophotometer, with a spectral resolution of 1 nm with an associated instrumental error of ± 0.5 nm. The method used to measure the absorption coefficient of phytoplankton was the modified opal glass technique, which measures the absorption of whole phytoplankton on a filter pad. It is possible to measure the absorption of the pigments contained in the phytoplankton by subtracting the absorption spectra of the filter paper after processing in methanol (Kishino *et al.* 1985).

The fourth-derivative method was applied to the absorption spectra of the natural samples, resulting in peaks at 12 wavelengths (see the second column of table 5a). Pigment analysis (HPLC) showed the presence of a number of different biomarkers (table 5b). The group of pigments chlorophyll-*a*, fucoxanthin, chlorophyll-*c* and

diadinoxanthin indicate the presence of diatoms and/or coccolithophorides; chlorophyll-*b* means green algae; peridinin denotes the presence of photosynthetic dinoflagellates and zeaxanthin marks the presence of blue–green algae (Jeffrey 1980, Kirk 1983, Prézelin and Bóczar 1986).

Band 1, centred at 400 nm may be due to either chlorophyll-*a* derivatives or to non-photosynthetic pigments. The peaks appearing at 428 and 674 nm are caused by the presence of chlorophyll-*a*. Peaks at 454, 588 and 630 nm can be assigned to chlorophyll-*c*, while the peak at 468 nm denotes the presence of chlorophyll-*b* (Bidigare *et al.* 1990).

Carotenoids completely dominate the region from 482–556 nm (peaks 5–9). Absorption due to zeaxanthin occurs at the peak centred at 482 nm. Fucoxanthin and its derivatives are responsible for the peaks appearing at 514, 530 and 556 nm. However, the fuxcoxanthin derivative pigment butoxyfucoxanthin (a photosynthetic active carotenoid) causes the large absorption at 494 nm (Rowan 1989, Bidigare *et al.* 1990, Hoepffner and Sathyendranath 1993).

Table 5a. Absorption peaks of mixed natural populations from 9 May 1995 derived from the fourth-derivative method and curve-fitting procedure, including proportions of Gaussian and Lorentzian weights.

No.	Original peak (nm)	Adjusted peak (nm)	Gaussian weight	Lorentzian weight
1	400	390.86	0.0426	0.0016
2	428	430.15	0.0696	0.0081
3	454	454.73	0.0379	0.0102
4	468	470.59	0.0348	0.0106
5	482	488.00	0.0272	0.0026
6	494	496.66	0.0217	0.0000
7	514	514.99	0.0148	0.0030
8	530	534.79	0.0138	0.0054
9	556	553.78	0.0098	0.0042
10	588	587.46	0.0115	0.0013
11	630	634.49	0.0143	0.0013
12	674	675.31	0.0336	0.0073

Table 5b. Pigment analysis (HPLC) showing pigments, their concentrations and retention times.

Pigment	Concentration ($\mu g l^{-1}$)	Retention time (min)
Chlorophyll-c_3	1.478	01.446
Peridinin	0.223	04.225
Butoxyfucoxanthin	32.394	05.850
Fucoxanthin	1.045	06.446
Hexoxyfucoxanthin	1.028	07.013
Diadinoxanthin	7.141	07.892
Alloxanthin	6.445	08.621
Zeaxanthin	0.226	09.208
Cholorphyll-*b*	3.244	11.638
Chlorophyll-*a*	110.330	12.583

3.9. *Gaussian–Lorentzian curves*

The method for the Voigt approximation described earlier was applied to the three types of absorption spectra—the *in vivo* monocultures, the solvent-extracted monocultures and the natural populations (*in vivo*)—using the spectral peaks obtained by the fourth-derivative analysis. The adjusted peaks and the Gaussian and Lorentzian weightings of *in vivo* algal groups are shown in tables 3a and 3b; results for acetone-extracted samples are shown in tables 4a and 4b; and results for natural populations are presented in table 5a.

Figures 3(*a*) and 3(*b*), 4(*a*) and 4(*c*) and 5 show examples of the convoluted spectra compared to the measured spectra, and also show the shape of the component spectra for each peak. The figures show a good fit for all the examples, whether the samples were *in vivo* monocultures ($r = 0.979$, *Phaeodactylum tricornotum*; $r = 0.989$, *Tetraselmis suecica*) or solvent-extracted monocultures ($r = 0.995$, *Phaeodactylum tricornotum*; $r = 0.999$, *Synechococcus* sp.) or *in vivo* natural populations ($r = 0.998$).

These results show the effectiveness of the Voigt approach to simulate absorption spectra from known spectral peaks. It is important to note that the iterative process results in changes in the peak location. This is particularly true for the *in vivo* samples (see tables 3a and 5a and figures 3(*a*) and 3(*b*) and 5), but less so for the solvent-extracted samples.

4. Discussion

The results presented here demonstrate the use of derivative analysis to identify accurately spectral peaks caused by light absorbing pigments. They also show that it is more difficult to obtain information from the absorption spectra of intact phytoplankton than from solvent-extracted pigments. This is because the optical signal is masked by the light absorbing and scattering properties of the cell wall and contents.

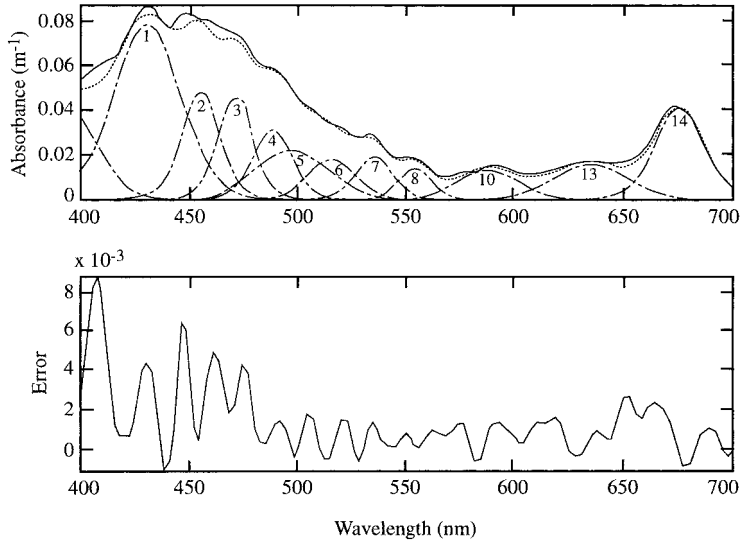

Figure 5. Absorption spectrum of natural populations collected on 9 May 1995, close to Plymouth, and the Gaussian–Lorentzian reconstruction; the bottom panel shows the magnitude of the error between the two curves.

The method was tested using theoretical absorption spectra constructed using the combined spectra of a number of pigments, whose spectral absorption was known, resulting in accurate identification of the pigments by attributing them to the obtained peaks. In this study typical spectra for two taxonomic groups, diatoms and green algae, were used.

The derivative analysis described can be used to identify spectral peaks in algal monocultures, for both acetone-extracted and *in vivo* samples. The individual absorption spectra of the component pigments, analysed by HPLC, were combined to model the absorption spectrum of the algal culture. There was good agreement between the modelled spectrum and the measured spectrum for the acetone-extracted samples. This can be partly explained by the fact that when component pigment absorption spectra are measured in acetone or other solvent, there is a spectral shift from the absorption characteristics in water. However, it is also the case that biliproteins were not extracted and so do not appear in the modelled results, although they are present in *Synechococcus* sp.

When the derivative method is simply used to identify peaks, and the ratio of the Gaussian or Lorentzian fit of the individual peaks is maximized, there is a good fit between the measured and the modelled spectra. There is some indication that the Gaussian fit is more appropriate at shorter wavelengths, and the Lorentzian fit improves relatively at longer wavelengths. This seems appropriate since the signal from pigments in the red part of the spectrum is more defined than that from the blue (French *et al.* 1972).

The work on natural populations also shows encouraging results. The fourth-derivative method identifies the spectral peaks, and curve fitting using the Gaussian–Lorentzian technique provides a close match to the original absorption spectrum. However, the information from the pigments is more difficult to match with the absorption spectrum. This is partly due to the mixture of phytoplankton studied. This has also previously been observed by Jeffrey (1997), who noted that optical techniques using hyperspectral data to identify phytoplankton taxonomic groups would be more useful in a monospecific algal bloom than in mixtures of phytoplankton.

Since information at the taxonomic level is useful, the characterization of biomarkers that are specific to particular groups of phytoplankton will be a valuable tool. For example, as we have shown here, chlorophyll-*b* can be used as a marker for chlorophytes, fucoxanthin can be used as a marker for diatoms, and chlorophyll-*c* can be used as a marker for diatoms and prymnesiophytes. The relative proportions of these biomarkers may also be used as a means of identification. This will be particularly true when satellite and airborne ocean colour sensors can provide data of higher spectral resolution (e.g. Moderate Resolution Imaging Spectroradiometer (MODIS) and MERIS).

Acknowledgments

We thank Dr Nicholas Hoepffner for providing us with a copy of the program used for determining the Gaussian or Lorentzian characteristics of absorption spectra and Dr Luis Proenca for his assistance in the HPLC analysis. Dr J. Aiken and Mr Guy Westbrook are gratefully acknowledged for their assistance in fieldwork carried out at Plymouth Marine Laboratory. We also thank Kate Davis for preparing the figures.

References

Banwell, C. N., 1972, *Fundamentals of Molecular Spectroscopy*, Third Edition (london: McGraw-Hill).

Barlow, R. G., Mantoura, R. F. C., Gough, M. A., and Fileman, T. W., 1993, Pigment signatures of the phytoplankton composition in the northeastern Atlantic during the 1990 spring bloom. *Deep-Sea Research*, **40**, 459–477.

Bidigare, R. R., Morrow, J. H., and Kiefer, D. A., 1989, Derivative analysis of spectral absorption by photosynthetic pigments in the western Sargasso Sea. *Journal of Marine Research*, **47**, 323–341.

Bidigare, R. R., Ondrusek, M. E., Morrow, J. H., and Kiefer, D. A., 1990, *In vivo* absorption properties of algal pigments. *Proceedings SPIE, Ocean Optics X*, **1302**, 290–302.

Bohren, C. F., and Huffman, D. R., 1983, *Absorption and Scattering of Light by Small Particles* (New York: Wiley).

Boldeskul, A. E., Buyan, G. P., Kondilenko, I. I., Novichenko, V. N., and Pogorelov, V. E., 1971, *Optical Spectroscopy*, **31**, 306–308.

Boney, A. D., 1976, *Phytoplankton. Studies in Biology*, 52 (London: Edward Arnold).

Bricaud, A., and Morel, A., 1986, Light attenuation and scattering of phytoplanktonic cells: a theoretical modelling. *Applied Optics*, **25**, 571–580.

Bricaud, A., Morel, A., and Prieur, L., 1983, Optical efficiency factors for some phytoplankters. *Limnology and Oceanography*, **28**, 816–832.

Butler, W. L., and Hopkins, D. W., 1970, Higher derivative analysis of complex absorption spectra. *Photochemistry and Photobiology*, **12**, 439–450.

Dexter, D. L., and Knox, R. S., 1965, *Excitons* (New York: Wiley Interscience).

French, C. S., Brown, J. S., and Lawrence, M. C., 1972, Four universal forms of chlorophyll-*a*. *Plant Physiology*, **49**, 421–429.

French, C. S., Brown, J. S., Prager, L., and Lawrence, M. C., 1969, Analysis of spectra of natural chlorophyll complexes. *Carnegie Institute Washington Yearbook*, **67**, 536–546.

Goedheer, J. C., 1970, On the pigment system of brown algae. *Photosynthetica*, **4**, 97–106.

Gordon, H. R., Clark, D. K., Brown, J. W., Brown, O. B., Evans, R. H., and Broenkow, W. W., 1983, Phytoplankton pigment concentrations in the Middle Atlantic Bight: comparison of ship determinations and CZCS estimates. *Applied Optics*, **22**, 20–36.

Gugliemelli, L. A., Dutton, H. J., Juursinic, P. A., and Siegelman, H. W., 1981, Energy transfer in a light-harvesting carotenoid–chlorophyll *c*–chlorophyll *a* protein of *Phaeodactylum tricornotum*. *Photochemistry and Photobiology*, **33**, 903–907.

Gulyayev, B. A., and Litvin, F. F., 1970, First and second derivatives of the absorption spectrum of chlorophyll and associated pigments in cells of higher plants and algae at 20°C. *Biofizika*, **15**, 701–712.

Hoepffner, N., and Sathyendranath, S., 1991, Effect of pigment composition on absorption properties of phytoplankton. *Marine Ecology Progress Series*, **73**, 11–23.

Hoepffner, N., and Sathyendranath, S., 1993, Determination of the major groups of phytoplankton pigments from the absorption spectra of total particulate matter. *Journal of Geophysical Research*, **98**, 22789–22803.

Jeffrey, S. W., 1976, The occurrence of chlorophyll c_1 and c_2 in algae. *Journal of Phycology*, **12**, 349–354.

Jeffrey, S. W., 1980, Algal pigments systems. In *Primary Production in the Sea*, edited by P. Falkowski (New York: Plenum), pp. 33–58.

Jeffrey, S. W., 1997, Applications of pigment methods to oceanography. In *Phytoplankton Pigments in Oceanography*, edited by S. W. Jeffrey, R. F. C. Mantoura and S. W. Wright (Paris: UNESCO, SCOR).

Kirk. J. T. O., 1983, *Light and Photosynthesis in Aquatic Ecosystems* (Cambridge: Cambridge University Press).

Kirk, J. T. O., and Tilney-Bassett, R. A. E., 1978, *The Plastids* (Amsterdam: Elsevier).

Kishino, M., Takahashi, M., Okami, N., and Ichimura, S., 1985, Estimation of the spectral absorption coefficients of phytoplankton in the sea. *Bulletin of Marine Science*, **37**, 634–642.

Lewis, M. R., Warnock, R. E., and Platt, T., 1985, Absorption and photosynthetic action

spectra for natural phytoplankton populations: Implications for production in the open ocean. *Limnology and Oceanography*, **30**, 794–806.

Mann, J. E., and Myers, M., 1968, On pigments growth and photosynthesis of *Phaeodactylum tricornotum*. *Journal of Phycology*, **4**, 349–355.

Mantoura, R. F. C., and Llewellyn, C. A., 1983, The rapid determination of algal chlorophyll and carotenoid pigments and their breakdown products in natural waters by reverse-phase high-performance liquid chromatography. *Analytica Chimica Acta*, **151**, 297–314.

Mitchell, A. C., and Zemansky, M. W., 1934, *Resonance Radiation and Excited Atoms* (Cambridge: Cambridge University Press).

Morel, A., and Bricaud, A., 1981, Theoretical results concerning light absorption in a discrete medium and application to specific absorption of phytoplankton. *Deep-Sea Research*, **28**, 1375–1393.

Prèzelin, B. B., 1980, Light reactions in photosynthesis. *Canadian Bulletin of Fisheries and Aquatic Science*, **210**, 1–43.

Prèzelin, B. B., and Bòczar, A. A., 1986, Molecular bases of cell absorption and fluorescence in phytoplankton: potential applications to studies in optical oceanography. In *Progress in Phycological Research*, Volume 4, edited by F. E. Round and D. J. Chapman (Bristol: Biopress), pp. 349–464.

Rees, W. G., 1990, *Physical Principles of Remote Sensing* (Cambridge: Cambridge University Press).

Rowan, K. S., 1989, *Photosynthetic Pigments of Algae* (Cambridge: Cambridge University Press).

Sathyendranath, S., Lazzara, L., and Prieur, L., 1987, Variations in the spectral values of specific absorption of phytoplankton. *Limnology and Oceanography*, **32**, 403–415.

Sauer, K., 1975, Primary events and the trapping of energy. In *Bioenergetics of Photosynthesis*, edited by Govindjee (New York: Academic Press).

Schanda, E., 1986, *Physical Fundamentals of Remote Sensing* (Berlin: Springer-Verlag).

Sundius, T., 1973, Computer fitting of Voigt profiles to Raman lines. *Journal of Raman Spectroscopy*, **1**, 471–488.

Thorne, A. A., 1974, *Spectrophysics* (London: Chapman and Hall).

Yokohama, Y., and Misonou, T., 1980, Chlorophyll *a*:*b* ratios in marine benthic green algae. *Japanese Journal of Phycology*, **28**, 219–223.